Published in final edited form as:
Biomaterials. 2011 February ; 32(5): 1361–1369. doi:10.1016/j.biomaterials.2010.10.043.

Combinatorial screening of osteoblast response to 3D calcium phosphate/poly(ε-caprolactone) scaffolds using gradients and arrays

Kaushik Chatterjee[a,b], **Limin Sun**[c], **Laurence C. Chow**[c], **Marian F. Young**[b], and **Carl G. Simon Jr.**[a,*]

[a]Polymers Division, National Institute of Standards and Technology, 100 Bureau Drive, Gaithersburg, MD 20899, USA

[b]Craniofacial and Skeletal Diseases Branch, National Institute of Dental and Craniofacial Research, National Institutes of Health, Bethesda, MD, USA

[c]American Dental Association Foundation, Paffenbarger Research Center, National Institute of Standards and Technology, Gaithersburg, MD, USA

Abstract

There is a need for combinatorial and high-throughput methods for screening cell–biomaterial interactions to maximize tissue generation in scaffolds. Current methods employ a flat two-dimensional (2D) format even though three-dimensional (3D) scaffolds are more representative of the tissue environment in vivo and cells are responsive to topographical differences of 2D substrates and 3D scaffolds. Thus, combinatorial libraries of 3D porous scaffolds were developed and used to screen the effect of nano-amorphous calcium phosphate (nACP) particles on osteoblast response. Increasing nACP content in poly (ε-caprolactone) (PCL) scaffolds promoted osteoblast adhesion and proliferation. The nACP-containing scaffolds released calcium and phosphate ions which are known to activate osteoblast function. Scaffold libraries were fabricated in two formats, gradients and arrays, and the magnitude of the effect of nACP on osteoblast proliferation was greater for arrays than gradients. The enhanced response in arrays can be explained by differences in cell culture designs, diffusional effects and differences in the ratio of "scaffold mass to culture medium". These results introduce a gradient library approach for screening large pore 3D scaffolds and demonstrate that inclusion of the nACP particles enhances osteoblast proliferation in 3D scaffolds. Further, comparison of gradients and arrays suggests that gradients were more sensitive for detecting effects of scaffold composition on cell adhesion (short time points, 1 day) whereas arrays were more sensitive at detecting effects on cell proliferation (longer time points, 14 day).

Keywords

3D scaffolds; Calcium phosphate; Combinatorial screening; Nanoparticles; Osteoblast; Tissue engineering

1. Introduction

There is a need to develop methods for systematic and rapid screening of cell–biomaterial interactions to identify optimal scaffold properties to maximize tissue generation. Previous

*Corresponding author. Tel.: +1 301 975 8574; fax: +1 301 975 4977. carl.simon@nist.gov (C.G. Simon).

methods for combinatorial screening of cell–material interactions have been developed where materials are presented to cells in a two-dimensional (2D) format [1–7]. For instance, polymer blend, surface chemistry and topography gradients have been fabricated for screening cell response to biomaterials [3,5,6]. An integrated platform for high-throughput polymer synthesis and protein-material-cell interaction assays was developed to screen human embryonic stem cell response to a large library consisting of 496 polymers [8]. In recent work, polymer arrays were fabricated by blending different combinations and ratios of 7 polymers into 135 binary polymer blends to screen osteoblast function [9].

These methods typically employ a flat 2D culture format. However, cells exist in a three-dimensional (3D) extracellular matrix in vivo. Therefore, when cultured in 3D scaffolds, cell response is more representative of their behavior in vivo [10–12]. Furthermore, biomaterials are commonly fabricated into 3D scaffolds for tissue engineering applications and cells are responsive to topographical differences between 2D substrates and 3D scaffolds [13]. Thus, there is a need to develop combinatorial methods for screening cell–material interactions using biomaterial array and gradient libraries where the materials are presented to cells in a 3D scaffold format.

Previously we reported a combinatorial approach for screening cell–material interactions in 3D scaffolds using an *array* approach [14]. Herein, we present a new *gradient* approach for fabricating scaffold libraries and perform experiments to directly compare the gradient and array formats. A bone tissue engineering model was used since there is strong need to develop synthetic bone graft therapies [15–17]. Poly(ε-caprolactone) (PCL) was used to fabricate scaffolds since it has been advanced for orthopaedic applications [18]. The MC3T3-E1 osteoblast cell line was used as a model for osteoblasts because it is a well-characterized and established model for in vitro studies [19,20]. The libraries were used to screen osteoblast response to PCL composite scaffolds containing amorphous calcium phosphate nanoparticles (nACP) prepared by spray-drying process [21], which have not been tested for potential tissue engineering applications.

Calcium phosphates (CaP) are the major inorganic component of bone and different forms of CaP have been used extensively in bone tissue engineering scaffolds [22–27]. For example, composite scaffolds of polyamide incorporating hydroxyapatite (HA) nanoparticles exhibited excellent biocompatibility in vitro and osteo-conductivity in vivo [23]. Findings of a 7-year clinical study indicate excellent outcomes when 3D porous HA scaffolds seeded with patient's bone marrow stromal cells were implanted as graft substitutes to repair long bone defects [25]. Self-setting calcium phosphate cements prepared from tetracalcium phosphate and dicalcium phosphate have been used to fabricate porous 3D tissue scaffolds [26]. Subcutaneous transplantation of a human bone marrow stromal cell suspension mixed with HA and tricalcium phosphate particles was shown to yield mature bone tissue in mice [27].

One of the most well-characterized mechanisms of action for CaP biomaterials is the release of calcium and phosphate ions to activate osteoblast function [28,29]. Osteoblasts express a calcium receptor, calcium ions stimulate osteoblast proliferation [28] and phosphate ions stimulate osteoblast differentiation [29]. nACP screened herein was chosen since its amorphous structure and nano-scale particle size were expected to enhance release of calcium and phosphate ions to activate osteoblasts. Amorphous CaP are known to be more soluble than other crystalline forms of CaP for a given Ca:P ratio and nanoparticles have high surface area to facilitate diffusion and ion release [22]. Thus, combinatorial gradients and arrays were used to screen the effect of nACP content in 3D scaffolds on osteoblast adhesion and proliferation.

2. Materials and methods

2.1. Preparation and characterization of nACP particles

nACP particles with Ca:P ratio of 1.5 were prepared by the spray-drying process reported previously [21]. Briefly, calcium carbonate and dicalcium phosphate were dissolved in acetic acid solution at a Ca:P M ratio of 1.5. The solution was sprayed through a nozzle placed on top of a heated glass column. Filtered dry air was supplied from the top of the column and an electrostatic precipitator connected to the lower end of the column drew air from the column creating a steady flow of mist through the column. Water and volatile acids in the solution were removed with the air flow while the fine particles suspended in the air flow were collected by the precipitator. For transmission electron microscopy (TEM, JEOL), nACP particles were deposited from a dilute solution in acetone on to an amorphous carbon film supported by a Cu grid. X-ray diffraction (XRD, DMAX 220, Rigaku Denki) was used to determine the crystal structure of the nanoparticles. Scans were performed between $10° < 2\theta < 50°$. Highly crystalline Reference Material hydroxyapatite (HA) powder was obtained from the National Institute of Standards and Technology [30] and used for comparison in XRD. To assess the change in the crystallinity of the nACP during exposure to water, nACP particles were incubated in excess water for 4 d, air dried and examined by XRD.

2.2. Fabrication of scaffold libraries

A combinatorial platform was adapted to prepare scaffold libraries in the form of arrays and gradients [14,31]. Two polymer solutions containing total of 0.1 g solids per mL of dioxane were prepared consisting of either pure PCL (65000 g/mol relative molecular mass, Sigma) or PCL solution containing 30 mass % nACP (hereafter 30% nACP-PCL). The two solutions were drawn into two syringes and placed on opposing syringe pumps (New Era NE-1000) connected to the inlet port of a static mixer using a T-junction connector. The pumps were programmed such that the output from the PCL syringe decreased linearly from 0.5 mL/min to 0 mL/min as the flow from the PCL-nHA syringe increased from 0 mL/min to 0.5 mL/min. Thus, the effluent from the stasssstic mixer was maintained constant at 0.5 mL/min even as it progressively changed from PCL-rich to nACP-rich with time. The effluent was deposited drop-wise onto a Teflon trough (75 mm long × 8 mm wide × 6 mm deep) containing 4.3 g of sieved NaCl crystals (250 μm–425 μm in diameter). A stainless steel wire was placed length-wise in the center of the salt trough to facilitate handling of the completed gradient scaffolds after fabrication. The Teflon mold was placed on a motorized stage which was programmed to translate the trough (75 mm/2 min) during deposition of the effluent from the static mixture to generate a composition gradient along the length of the salt trough.

The same apparatus was used for the array libraries except that effluent was collected into wells of a 96-well flat-bottom polypropylene plate containing 0.13 g of sieved NaCl in the wells. Two drops of the effluent from the static mixture was manually collected in each of the 36 wells to generate an array library (30 μL/well).

After gradient or array deposition, the libraries were frozen by immersion in liquid nitrogen and the solvent was removed by lyophilization. Salt from the scaffold libraries was leached in excess water for 4 d with daily water changes. The scaffold libraries were air dried and stored under vacuum until use. Scaffolds of uniform composition in both array and gradient formats were prepared as controls.

Control scaffolds of uniform composition with gradient or array geometries were fabricated in some cases. Controls were prepared using the same protocols described above except that pure PCL or only nACP-PCL solutions were used as appropriate. For characterization of nACP present in scaffolds (for XRD or ion release), control 30% nACP-PCL gradient

scaffolds were dissolved in dioxane and the particles were collected by centrifugation and air dried.

2.3. Scaffold characterization

The nACP content of scaffold libraries was determined by thermogravimetric analysis (TGA) by heating in a Pt pan at 20 °C/min in air. For gradients, scaffolds were cut into 7 segments for TGA. For arrays, 5 wells were analyzed out of 36 (wells 1, 9, 18, 27 and 36). Control runs in nitrogen indicated there were no significant differences in TGA profiles in air and nitrogen. To assess nACP lost during scaffold fabrication, drops of effluent from the scaffold fabrication apparatus were collected on a glass slide and allowed to air dry into thick films. The films were easily peeled off the slides for TGA analysis. Percent mass remaining at 533 °C was used for all TGA analysis and calculations. For scanning electron microscopy (SEM), scaffolds were sputter-coated with gold and imaged (15 kV, Hitachi S-4700-II FE-SEM). For mechanical testing, uni-axial static compressive load was applied (0.03 mm/s) by a Dynamic Mechanical Analyzer (TA Instruments) to control array scaffolds of pure PCL and 30% nACP-PCL. The slope of the linear fit to the stress-strain plot for (5–10) % strain was taken as the measure of compressive modulus.

2.4. Calcium and phosphate ion release

Release of calcium and phosphate ions from calcium phosphate particles was measured in an aqueous buffer containing 133 mmol/L NaCl and 50 mmol/L HEPES at pH 7.4 [32]. Particles (5 mg of nACP, HA or nACP extracted from 30% nACP-PCL scaffolds) were suspended in buffer (1 mL) and stirred for 15 min at 37 °C. For ion release from scaffolds, eight array scaffolds of pure PCL or 30% nACP-PCL were used in 1 mL of buffer. Solutions were centrifuged to remove suspended particles before measurement of ions in the supernatant. The concentration of soluble calcium and phosphate ions in the supernatant was determined using previously-reported spectrophotometric methods using O-(1,8-dihydroxy-3,6-disulfon-aphthylene-2,7-bisazo)-bisbenzenearsonic acid and malachite green molybdate tetrahydrate reagents for calcium and phosphate, respectively [33].

2.5. Cell culture

MC3T3-E1 cells (Riken Cell Bank, Japan), a well-characterized osteoblast model [19,20], were used to screen the scaffold libraries. Cells were cultured in media prepared from α-modification of Eagle's minimum essential medium (Invitrogen) supplemented with 10% volume fraction of fetal bovine serum (Gibco) and 0.6% volume fraction of kanamycin sulfate (Sigma–Aldrich), as described previously [14,34]. Passage 4 cells at 80% confluency were used for all experiments.

To culture cells in the gradient scaffolds, a rig was prepared by assembling four pieces of Teflon in a 15 cm diameter tissue culture polystyrene dish. The rigs were machined to yield a central cavity of 8 cm × 5 cm × 2 cm (Fig. 2c). Small holes were drilled into the walls of the Teflon rigs so that the wire placed in the middle of the gradients could be inserted to suspend the gradients slightly above the bottom of the dishes. Three gradient scaffolds were arranged in each dish as shown in Fig. 2 c. The array scaffolds in the 96-well plate were used as prepared by adding cells and medium to the tops of the scaffolds in the wells.

Scaffold libraries were sterilized with ethylene oxide (Anderson Products) and placed under vacuum to degas for 3 d. To wet gradient scaffold pores with medium, 50 mL of cell culture medium was added to each plate and plates were exposed to house vacuum. The medium was replaced with 80 mL of fresh medium containing 2 10^6 MC3T3-E1 cells. Note that the medium was added to the plate away from the scaffolds and was allowed to gently rise and fill the dish to allow for uniform cell settling along the gradients. A similar procedure was

followed for the array libraries except that 0.2 mL medium was added to each scaffold prior to applying vacuum. The media was then replaced by 0.2 mL of fresh medium containing 5000 cells in each well. All scaffolds were left undisturbed for 1 h immediately after cell seeding before they were transferred to an incubator to allow cells to make initial attachments. Media was refreshed every 3 d–4 d.

2.6. Soluble DNA assay

Picogreen dsDNA Quantitation kit (Molecular Probes) was used to determine the amount of DNA on the scaffolds as a measure of the number of cells at 1 d and 14 d after seeding. For gradients, libraries were cut into 7 segments (1 cm) along the gradient using a sharp razor. The segments were separated from the wire and incubated in 1 mL lysis solution from the kit containing 0.02 mass % sodium dodecyl sulfate (SDS) and 0.2 mg/mL Proteinase K for 24 h at 37 °C in 24-well plates. For arrays, lysis solution (0.2 mL) was added directly to scaffolds in the plates. Cell lysate (0.1 mL) from gradients and arrays was transferred to a fresh 96-well plate with 0.1 mL of Picogreen dye solution. Fluorescence intensity was measured by a micro-plate reader using excitation 488 nm and emission 525 nm, respectively. A calibration plot prepared from serial dilutions of a supplier-provided DNA solution was used to calibrate readings. A total of 8 arrays were used for cell experiments using 4 for each time point (1 d and 14 d). Every third well of the arrays was used for DNA assay and the remaining wells were for fluorescence microscopy. A total of 12 gradients were used for cell experiments where 4 were used for DNA assay and 2 were used for fluorescence microscopy at each time point.

2.7. Fluorescence microscopy

Cells in scaffolds were fixed with 3.7% formaldehyde in 0.1 mol/L phosphate buffered saline (PBS) for 15 min at 37 °C, permeabilized in 0.2% Triton X-100 for 5 min at 37 °C and stained with 1 μmol/L Sytox green (Invitrogen) solution in PBS for 1 h at 37 °C. Stained cells were imaged using an inverted epifluorescence microscope (Nikon Eclipse TE 300) in the green channel.

3. Results

The objective of this study was to prepare combinatorial scaffold libraries for screening the effect of nACP content in PCL scaffolds on osteoblast adhesion and proliferation in 3D. TEM showed the nACP used herein consisted of spherical nanoparticles with approximate diameter 100 nm (Fig. 1a) whereas XRD indicated that the nACP was amorphous (Fig. 1b). A broad peak in the spectra for 25°–35° is typical of an amorphous phase relative to the sharp peaks observed for crystalline HA (Fig. 1b). A static mixer-based platform was used to fabricate salt-leached scaffold libraries in gradient and array formats (Fig. 2). The scaffolds were composed of PCL and libraries had systematically varied nACP content.

TGA was used to determine nACP composition in scaffold libraries since polymers degrade at lower temperatures than ceramics (Fig. 3a). Control PCL scaffolds degraded completely at 533 °C (1% mass remaining). Control nACP particles lost 24% of their original mass when heated which was attributed to loss of moisture and lattice water. Control 30% nACP-PCL scaffolds retained 18% of their original mass. This value was back-corrected to account for the moisture mass loss of nACP particles to reveal that the 30% nACP-PCL scaffolds contained 24% nACP particles after fabrication and salt-leaching (18%/0.76 24%) (Fig. 3b). To determine the amount of nACP that was lost from scaffolds during salt-leaching, TGA was run on a dried polymer film formed by depositing 30 μL of 30% nACP-PCL solution onto a glass slide. When back-corrected for the mass loss of nACP particles, the films were found to contain 31% nACP (Fig. 3b). These results indicate that the control scaffolds

contained 31% nACP prior to salt-leaching but only 24% nACP after salt-leaching, that is, 23% of the initial nACP content was lost from the scaffolds during salt leach. Using this TGA with correction for nACP mass loss, composition of gradient libraries was observed to increase linearly in nACP content from 1% at the PCL-rich end to 14% at the nACP-rich (Fig. 3c). The nACP content in the arrays ranged from 3% to 23% for wells 1 to 36 (Fig. 3d). Thus, the 2-syringe pump approach yielded scaffold libraries with repeatable, linear variations in nACP content.

XRD indicated that nACP particles extracted from salt-leached scaffolds had become partially crystalline (small sharp peaks in spectra) relative to the amorphous nACP starting material (no sharp peaks) (Fig. 1b). For comparison, nACP particles incubated in water for 4 d (and air dried) were more crystalline than the nACP particles extracted from scaffolds. These data indicate that immersion in aqueous medium increases the crystallinity of nACP. The observation that nACP incubated in water is more crystalline than nACP from scaffolds suggests that incorporation of nACP in the scaffolds reduces nACP access to medium as some nACP particles may be completely encapsulated within the polymer in the walls of the pores of the scaffold.

Release of calcium and phosphate ions from nACP was measured (Fig. 4) since these ions are known to stimulate osteoblast function. nACP particles, nACP particles extracted from scaffolds, and control 30% nACP-PCL scaffolds released significant amounts of calcium and phosphate ions whereas control PCL scaffolds did not. These data indicated that nACP-PCL composite scaffolds can release calcium and phosphate ions into the aqueous medium. There was no significant difference (t-test, p 0.05, mean ± S.D.) in compressive moduli of control array scaffolds (PCL 32 kPa ± 6 kPa; 30% nACP-PCL 32 kPa ± 9 kPa). Thus, addition of nACP to scaffolds did not change bulk mechanical properties.

At 50× and 200× magnification in SEM, a similar scaffold structure was observed with and without nACP and for gradients and arrays (Fig. 5). Large pores (≈ 300 μm) visible at 50× result from NaCl porogen while smaller voids (≈ 10 μm) in the walls of the pores visible at 200× are from solvent evaporation/sublimation during freeze-drying [14]. At 50000×, nACP particles were visible on the scaffolds containing nACP. These data indicate gradients and arrays had similar scaffold structure and that nACP particles were present in nACP-PCL composite scaffolds.

DNA content at 1 d and 14 d in the scaffolds were taken as measures of cell adhesion and proliferation, respectively. MC3T3-E1 osteoblasts seeded onto gradient scaffold libraries adhered (1 d) more efficiently to scaffolds as nACP content increased (Fig. 6). For arrays, osteoblast adhesion (1 d) was the same for all scaffolds except the lowest nACP composition which dropped slightly. Osteoblast numbers at 14 d were enhanced with increasing nACP composition for both gradients and arrays but the magnitude of response was much higher for arrays. In addition, cell numbers at 14 d on arrays showed a sharp increase at 12% nACP. DNA measurements were corroborated by fluorescence imaging of cell nuclei (Fig. 7) where the effect of increased nACP content on cell numbers at 14 d was more pronounced for the arrays compared to gradients. Control osteoblast experiments were performed for gradient-shaped scaffolds that had uniform composition of pure PCL or 20% nACP-PCL (Supplementary Fig. S1) and osteoblasts numbers were higher on nACP-rich scaffolds at both 1 d and 7 d culture. These controls confirm that osteoblast behavior on the gradient libraries was not an artifact of the combinatorial format. The combinatorial screens indicate that addition of nACP to polymer scaffolds can enhance osteoblast adhesion and proliferation.

4. Discussion

Few combinatorial methods have been reported for screening cell–material interactions in 3D [14,34,35]. We previously reported an array approach for screening salt-leached polymer scaffolds that varied in polymer composition [14] and found that blends of pDTEc/pDTOc [poly(desaminotyrosyl-tyrosine ethyl ester carbonate)/poly (desaminotyrosyl-tyrosine octyl ester carbonate)] rich in pDTEc enhanced osteoblast proliferation. In more recent work, we introduced a combinatorial gradient approach for screening hydrogel scaffolds and used gradients in hydrogel modulus to demonstrate that stiffer gels induced osteogenesis in 3D [34]. 3D hydrogel scaffold arrays have been developed for screening human embryonic stem cell differentiation and particular combinations of extracellular matrix proteins were found to drive cells down osteogenic and endothelial lineages [35]. Herein, our previous work with salt-leached scaffold arrays [14] has been extended to introduce a new gradient approach.

Several differences in osteoblast response were observed between gradients and arrays (Fig. 6) that can be explained by a combination of the cell culture design and diffusional effects. For instance, cell numbers at 1 d increased monotonically with increasing nACP for gradients but were nearly the same for all compositions with arrays. For arrays, cells had only one option, which was to settle on the scaffold. The bottoms of the wells were completely occupied by the scaffolds such that cells had to land on the scaffolds. Cells seeded on array scaffolds were essentially “forced” to adhere to the scaffold such that differences in nACP composition were not able to influence adhesion. For gradients, cells had two options, to either land on the scaffolds or float away from the scaffolds to settle onto the bottom of the dish. The availability of two outcomes (adherence to scaffold or adherence to dish) made it possible for nACP to have an observable effect on adhesion (1 d) to scaffolds with the gradient library format. Thus, the gradient approach was more sensitive for detecting effects of scaffold composition on cell adhesion (short time points, 1 d).

At 14 d, osteoblast numbers were enhanced in PCL scaffolds containing nACP for both gradients and arrays, but the magnitude of enhancement was higher for arrays (Fig. 6). Furthermore, cell numbers at 14 d on arrays showed a biphasic response with a sharp increase at 12% nACP whereas a linear increase in cell numbers at 14 d was observed for gradients. For gradients, all scaffold compositions were in a single dish and shared the same 80 mL of medium. Thus, released calcium and phosphate ions could diffuse about the dish to stimulate osteoblasts at all gradient positions. This effect likely dampened differences in osteoblast proliferation between nACP-rich and nACP-poor segments of the gradients. For arrays, discrete scaffold compositions were in individual wells within 0.2 mL of medium. Thus, only the scaffolds within each well could release calcium and phosphate ions to activate osteoblasts. Under these conditions, osteoblasts on array scaffolds with low nACP content were not stimulated to proliferate (array scaffolds < 12% nACP in Fig. 6b). Calcium and phosphate ions released from array scaffolds containing higher nACP contents were concentrated in the 0.2 mL of medium in each well leading to stronger enhancement of proliferation (array scaffolds 12% nACP in Fig. 6b). The “scaffold mass (g) to culture medium volume (mL) ratio” for gradients was 0.00375 [(3 gradients per dish × 0.1 g per gradient)/80 mL medium] while the ratio was 0.15 for arrays [0.03 g per scaffold/0.2 mL medium]. Thus, arrays had a 40-fold higher ratio than gradients (0.15/0.00375). Lastly, the larger effect on cell number observed for arrays at 14 d may also have been influenced by compositional differences between arrays and gradients since the arrays included scaffolds with up to 23% nACP while the gradients only reached 14% nACP. In sum, gradients and arrays yielded the similar conclusions: that the nACP particles stimulated osteoblast adhesion and proliferation in polymer scaffolds. However, differences were observed between the two approaches that arose from differences in cell culture design and diffusional effects. Gradients were useful for detecting scaffold composition effects on cell adhesion at

short time points (1 d), but were not sensitive at detecting scaffold effects on cell proliferation at longer time points (14 d). Arrays were the opposite: insensitive to scaffold effects on adhesion but very sensitive to effects on proliferation.

For future work, the gradient approach could be modified to utilize less medium but diffusional effects of soluble factors will continue to play a role in influencing the biological response - a limitation of the gradient format. Although arrays exclude diffusional effects between scaffolds, they require significantly more handling during cell seeding and bioassays. There is only one dish for 3 gradient libraries while 3 array libraries is 108 wells (36×3). In addition, the salt-leached gradient scaffolds described herein can have application for engineering graded tissues [34,36–38]. Gradients are prevalent in vivo for directing tissue morphogenesis and for organogenesis where tissues are hierarchically organized and interfaced through transitional zones [39,40]. Specifically, ligaments and tendons join soft and hard tissues utilizing gradients from softer collagenous tissue into hard bony tissue [40]. The nACP gradients described herein could have application in this regard since they induced a graded osteoblast response.

5. Conclusions

A gradient approach for systematic screening of cell response to 3D scaffold composition has been presented using a salt-leached gradient scaffold approach. The gradient 3D scaffold library method was compared with a 3D array approach to identify differences between gradient and array techniques. Combinatorial screens were used to test the effect of nACP particles on osteoblast adhesion and proliferation. Scaffolds containing nACP enhanced osteoblast adhesion and proliferation, an effect which is explained by release of calcium and phosphate ions from nACP. Overall, results from gradient and array library formats were similar, but differences were observed that can be explained by effects of the cell culture designs on calcium and phosphate ion concentration and diffusion. Gradients were best for measuring effects of scaffold composition on cell adhesion at short time points while arrays were best for measuring scaffold effects on cell proliferation at longer time points. These results demonstrate a new combinatorial gradient approach for screening the effect of salt-leached scaffold composition on cell response in 3D.

Supplementary Material

Refer to Web version on PubMed Central for supplementary material.

Acknowledgments

K.C. acknowledges support from a Research Associateship Award from the National Research Council of the National Academy of Sciences in the Joint NIH-NIBIB/NIST Postdoctoral Program (National Institutes of Health-National Institute of Biomedical Imaging and Bioengineering/National Institute of Standards and Technology). This work was supported by NIST, the Intramural Program of the NIH-NIDCR (National Institute of Dental and Craniofacial Research), NIH-NIBIB R21 EB006497-01 and NIH-NIDCR R01DE16416. The standard deviation (S.D.) is the same as the “combined standard uncertainty of the mean” for the purposes of this work. The content is solely the responsibility of the authors and does not necessarily represent the official views of NIH, NIBIB, NIDCR, NIST or ADA (American Dental Association). This article, a contribution of NIST and NIH, is not subject to US copyright. Certain equipment and instruments or materials are identified in the paper to adequately specify the experimental details. Such identification does not imply recommendation by NIST, nor does it imply the materials are necessarily the best available for the purpose.

Appendix. Supplementary data

Supplementary data associated with this article can be found, in the online version, at doi: 10.1016/j.biomaterials.2010.10.043

Appendix

Figures with essential colour discrimination. Figs. 1, 3, 6 and 7 of this article have parts that are difficult to interpret in black and white. The full colour images can be found in the online version, at doi:10.1016/j.biomaterials.2010.10.043.

References

1. Simon CG, Yang Y, Thomas V, Dorsey SM, Morgan AW. Cell interactions with biomaterials gradients and arrays. Comb Chem High Throughput Screen. 2009; 12(6):544–553. [PubMed: 19601752]
2. Lin NJ, Lin-Gibson S. Osteoblast response to dimethacrylate composites varying in composition, conversion and roughness using a combinatorial approach. Biomaterials. 2009; 30(27):4480–4487. [PubMed: 19520423]
3. Yang J, Rose FRAJ, Gadegaard N, Alexander MR. A high-throughput assay of cell-surface interactions using topographical and chemical gradients. Adv Mater. 2009; 21(3):300–304.
4. Mei Y, Saha K, Bogatyrev SR, Yang J, Hook AL, Kalcioglu ZI, et al. Combinatorial development of biomaterials for clonal growth of human pluripotent stem cells. Nat Mater. 2010; 9(9):768–778. [PubMed: 20729850]
5. Meredith JC, Sormana JL, Keselowsky BG, Garcia AJ, Tona A, Karim A, et al. Combinatorial characterization of cell interactions with polymer surfaces. J Biomed Mater Res A. 2003; 66(3): 483–490. [PubMed: 12918030]
6. Simon J, Carl G, Eidelman N, Kennedy SB, Sehgal A, Khatri CA, et al. Combinatorial screening of cell proliferation on poly(l-lactic acid)/poly(d, l-lactic acid) blends. Biomaterials. 2005; 26(34): 6906–6915. [PubMed: 15939467]
7. Simon CG Jr, Lin-Gibson S. Combinatorial and high-throughput screening of biomaterials. Adv Mater. in press.
8. Mei Y, Gerecht S, Taylor M, Urquhart AJ, Bogatyrev SR, Cho S-W, et al. Mapping the interactions among biomaterials, adsorbed proteins, and human embryonic stem cells. Adv Mater. 2009; 21(27): 2781–2786.
9. Khan F, Tare RS, Kanczler JM, Oreffo ROC, Bradley M. Strategies for cell manipulation and skeletal tissue engineering using high-throughput polymer blend formulation and microarray techniques. Biomaterials. 2010; 31(8):2216–2228. [PubMed: 20056271]
10. Hall HG, Farson DA, Bissell MJ. Lumen formation by epithelial cell lines in response to collagen overlay: a morphogenetic model in culture. Proc Nat Acad Sci U S A. 1982; 79(15):4672–4676.
11. Abbott A. Cell culture: biology's new dimension. Nature. 2003; 424(6951):870–872. [PubMed: 12931155]
12. Cukierman E, Pankov R, Stevens DR, Yamada KM. Taking cell-matrix adhesions to the third dimension. Science. 2001; 294(5547):1708–1712. [PubMed: 11721053]
13. Dalby MJ, Gadegaard N, Tare R, Andar A, Riehle MO, Herzyk P, et al. The control of human mesenchymal cell differentiation using nanoscale symmetry and disorder. Nat Mater. 2007; 6(12): 997–1003. [PubMed: 17891143]
14. Yang Y, Bolikal D, Becker ML, Kohn J, Zeiger D, Simon CG Jr. Combinatorial polymer scaffold libraries for screening cell-biomaterial interactions in 3D. Adv Mater. 2008; 20(11):2037–2043.
15. Bostrom MPG, Seigerman DA. The clinical use of allografts, demineralized bone matrices, synthetic bone graft substitutes and osteoinductive growth factors: a survey study. HSS J. 2005; 1(1):9–18. [PubMed: 18751803]
16. Keating JF, McQueen MM. Substitutes for autologous bone graft in orthopaedic trauma. J Bone Jt Surg Br. 2001; 83-B(1):3–8.
17. Bueno EM, Glowacki J. Cell-free and cell-based approaches for bone regeneration. Nat Rev Rheumatol. 2009; 5(12):685–697. [PubMed: 19901916]
18. Savarino L, Baldini N, Greco M, Capitani O, Pinna S, Valentini S, et al. The performance of poly-[epsilon]-caprolactone scaffolds in a rabbit femur model with and without autologous stromal cells and BMP4. Biomaterials. 2007; 28(20):3101–3109. [PubMed: 17412415]

19. Sudo H, Kodama H, Amagai Y, Yamamoto S, Kasai S. In vitro differentiation and calcification in a new clonal osteogenic cell line derived from newborn mouse calvaria. J Cell Biol. 1983; 96(1): 191–198. [PubMed: 6826647]
20. Powell K, Leslie M. Dishing up bone formation. J Cell Biol. 2005; 171:409.
21. Chow LC, Sun LM, Hockey B. Properties of nanostructured hydroxyapatite prepared by a spray drying technique. J Res Natl Inst Stand Technol. 2004; 109(6):543–551.
22. Dorozhkin SV. Bioceramics of calcium orthophosphates. Biomaterials. 2010; 31(7):1465–1485. [PubMed: 19969343]
23. Wang H, Li Y, Zuo Y, Li J, Ma S, Cheng L. Biocompatibility and osteogenesis of biomimetic nano-hydroxyapatite/polyamide composite scaffolds for bone tissue engineering. Biomaterials. 2007; 28(22):3338–3348. [PubMed: 17481726]
24. Mastrogiacomo M, Scaglione S, Martinetti R, Dolcini L, Beltrame F, Cancedda R, et al. Role of scaffold internal structure on in vivo bone formation in macro-porous calcium phosphate bioceramics. Biomaterials. 2006; 27(17):3230–3237. [PubMed: 16488007]
25. Marcacci M, Kon E, Moukhachev V, Lavroukov A, Kutepov S, Quarto R, et al. Stem cells associated with macroporous bioceramics for long bone repair: 6-to 7-year outcome of a pilot clinical study. Tissue Eng. 2007; 13(5):947–955. [PubMed: 17484701]
26. Xu HHK, Weir MD, Simon CG. Injectable and strong nano-apatite scaffolds for cell/growth factor delivery and bone regeneration. Dent Mater. 2008; 24(9):1212–1222. [PubMed: 18359072]
27. Mankani MH, Kuznetsov SA, Marshall GW, Robey PG. Creation of new bone by the percutaneous injection of human bone marrow stromal cell and HA/TCP suspensions. Tissue Eng Part A. 2008; 14(12):1949–1958. [PubMed: 18800877]
28. Yamaguchi T, Chattopadhyay N, Kifor O, Sanders JL, Brown EM. Activation of p42/44 and p38 mitogen-activated protein kinases by extracellular calcium-sensing receptor agonists induces mitogenic responses in the mouse osteoblastic MC3T3-E1 cell line. Biochem Biophys Res Comm. 2000; 279(2):363–368. [PubMed: 11118293]
29. Beck GR, Zerler B, Moran E. Phosphate is a specific signal for induction of osteopontin gene expression. Proc Nat Acad Sci U S A. 2000; 97(15):8352–8357.
30. Markovic M, Fowler BO, Tung MS. Preparation and comprehensive characterization of a calcium hydroxyapatite reference material. J Res Natl Inst Stand Technol. 2004; 109(6):553–568.
31. Simon CG, Stephens JS, Dorsey SM, Becker ML. Fabrication of combinatorial polymer scaffold libraries. Rev Sci Instrum. 2007; 78 072207.
32. Xu HHK, Weir MD, Sun L, Takagi S, Chow LC. Effects of calcium phosphate nanoparticles on Ca-PO4 composite. J Dent Res. 2007; 86(4):378–383. [PubMed: 17384036]
33. Vogel GL, Chow LC, Brown WE. A microanalytical procedure for the determination of calcium, phosphate and fluoride in enamel biopsy samples. Caries Res. 1983; 17(1):23–31. [PubMed: 6571804]
34. Chatterjee K, Lin-Gibson S, Wallace WE, Parekh SH, Lee YJ, Cicerone MT, et al. The effect of 3D hydrogel scaffold modulus on osteoblast differentiation and mineralization revealed by combinatorial screening. Biomaterials. 2010; 31:5051–5062. [PubMed: 20378163]
35. Yang F, Cho S-W, Son SM, Hudson SP, Bogatyrev S, Keung L, et al. Combinatorial extracellular matrices for human embryonic stem cell differentiation in 3D. Biomacromolecules. 2010; 11(8): 1909–1914. [PubMed: 20614932]
36. Harley BA, Lynn AK, Wissner-Gross Z, Bonfield W, Yannas IV, Gibson LJ. Design of a multiphase osteochondral scaffold III: fabrication of layered scaffolds with continuous interfaces. J Biomed Mater Res Part A. 2010; 92A(3):1078–1093.
37. Phillips JE, Burns KL, Le Doux JM, Guldberg RE, Garcia AJ. Engineering graded tissue interfaces. Proc Nat Acad Sci U S A. 2008; 105(34):12170–12175.
38. Spalazzi JP, Doty SB, Moffat KL, Levine WN, Lu HH. Development of controlled matrix heterogeneity on a triphasic scaffold for orthopedic interface tissue engineering. Tissue Eng. 2006; 12(12):3497–3508. [PubMed: 17518686]
39. Lander AD. Morpheus unbound: reimagining the morphogen gradient. Cell. 2007; 128(2):245–256. [PubMed: 17254964]

40. Moffat KL, Sun W-HS, Pena PE, Chahine NO, Doty SB, Ateshian GA, et al. Characterization of the structure-function relationship at the ligament-to-bone interface. Proc Nat Acad Sci U S A. 2008; 105(23):7947–7952.

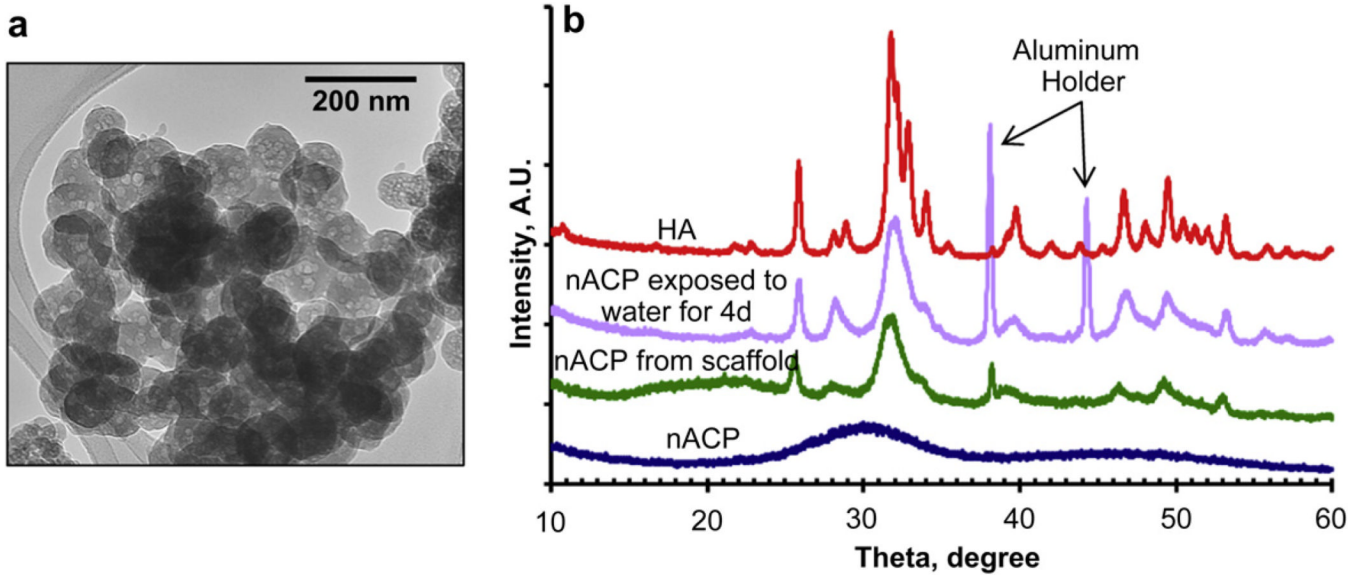

Fig. 1.

(a) TEM of nACP. (b) XRD spectra for nACP (blue), nACP collected from 30% nACP-PCL scaffolds (green), nACP particles after 4 d in water (purple), hydroxyapatite (red). Note that the peaks at 38.1° and 44.3° are characteristic of the aluminum sample holder.

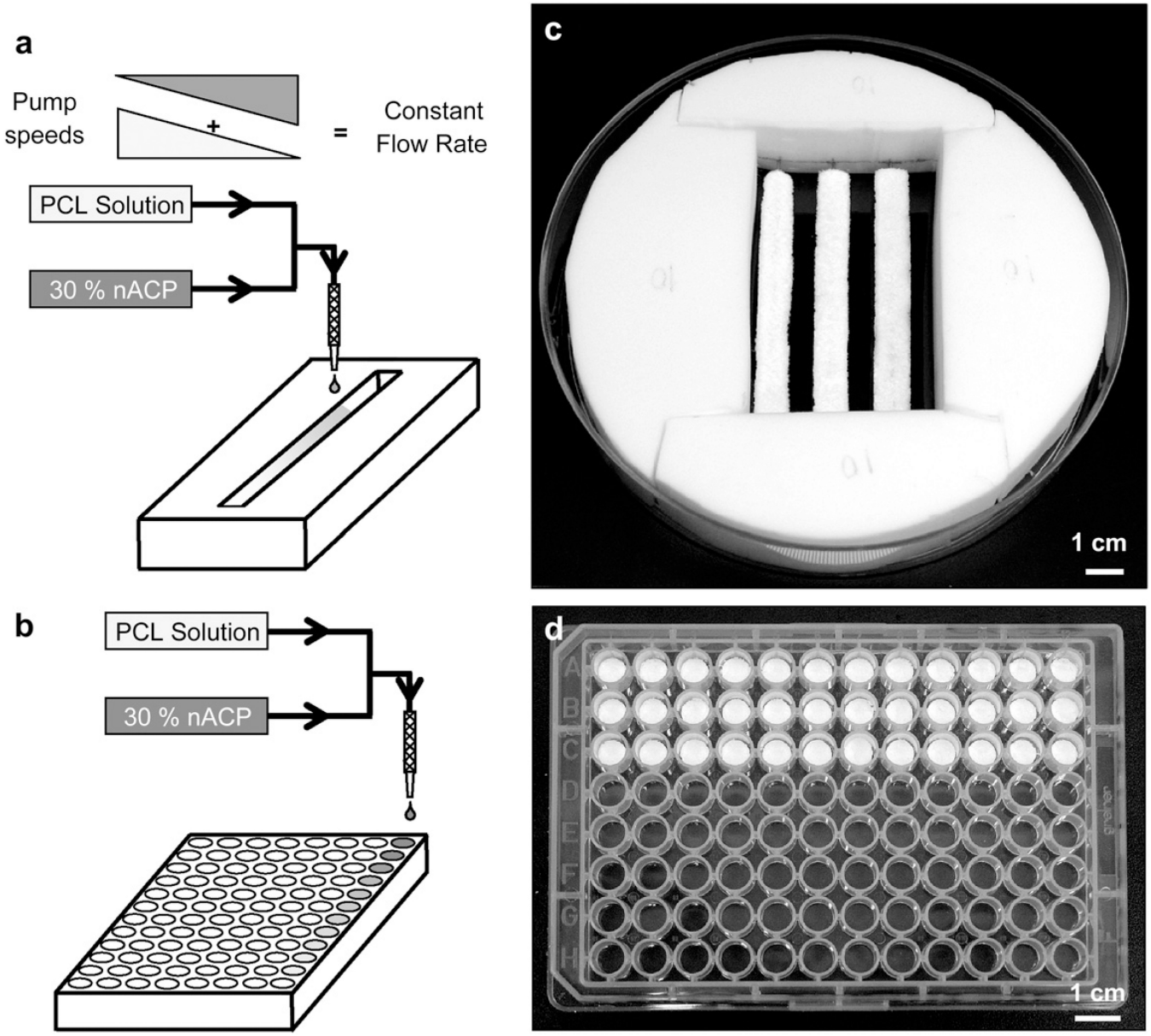

Fig. 2.

(a,b) Schematic representations of the combinatorial platforms used to fabricate the gradient (a) and array (b) scaffold libraries. Pure PCL solution and PCL solution with 30 mass % nACP particles were mixed and deposited onto a trough of NaCl porogen in either a continuous trough for gradients (a, c) or a 96-well plate for arrays (b, d). (c) Photograph of a Teflon rig supporting three gradient scaffold libraries in a 15 cm diameter dish used for cell culture. (d) Photograph of the scaffold arrays prepared in 96-well plates.

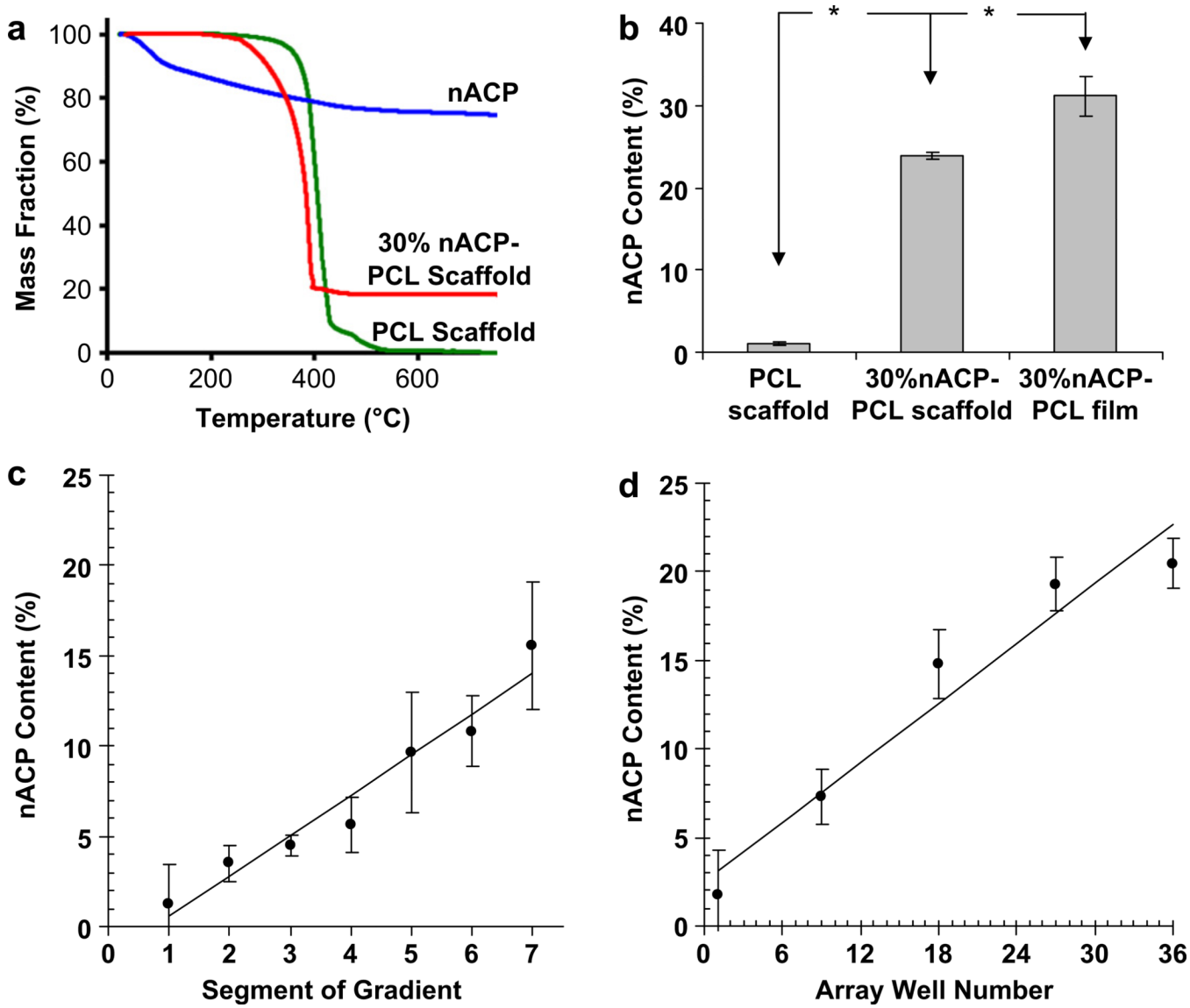

Fig. 3.

(a) TGA traces of nACP (blue), a control 30% nACP-PCL scaffold (red) and a control PCL scaffold (green). (b) Graph of CaP content determined by TGA for a control PCL scaffold, a control 30% nACP-PCL scaffold and a film of 30% nACP-PCL solution prepared on a glass slide. An asterisk encountered when following the line between two data points indicates that the data points are significantly different. (c, d) Plots of nACP content in the gradient (c) and array (d) libraries. All measurements in (b, c, d) are presented as mean ± S.D. for $n \geq 3$. (c, d) Both lines in (c, d) are linear fits with Pearson correlation coefficients (R) of 0.97.

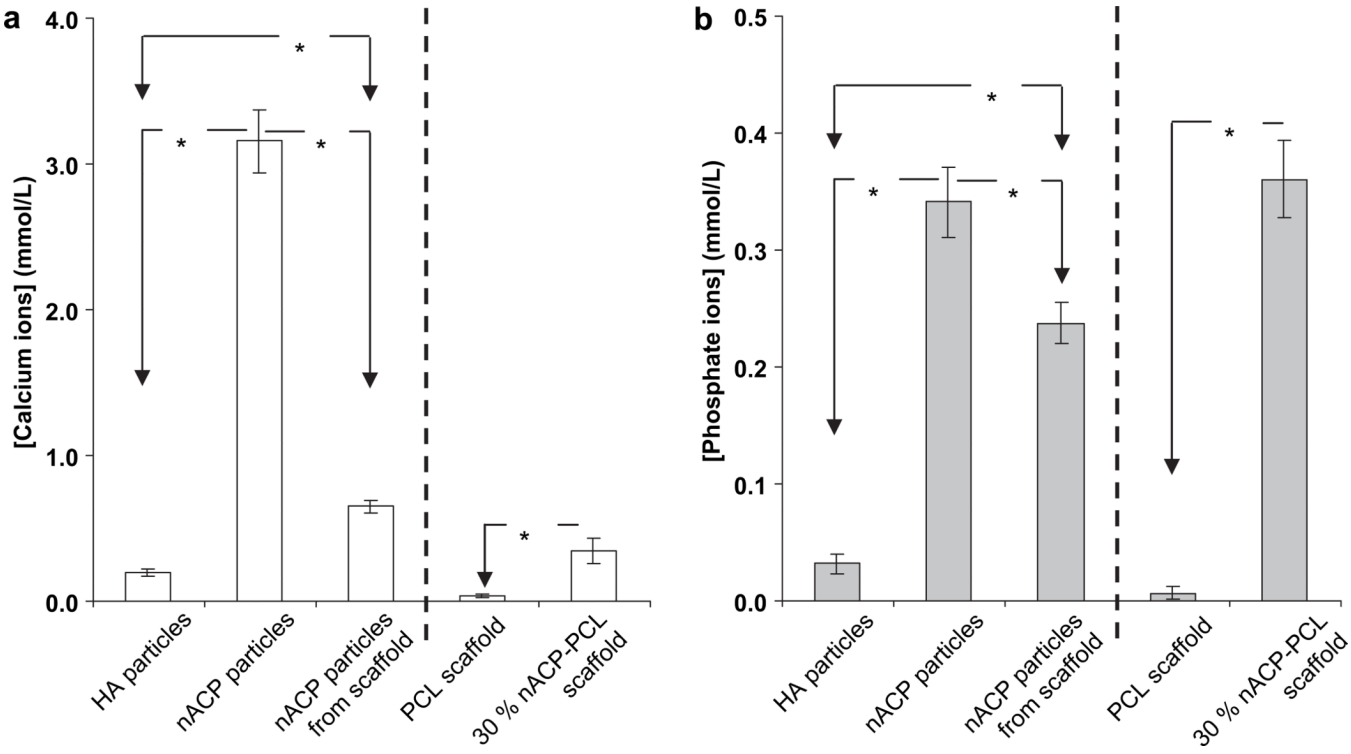

Fig. 4.

Release of (a) calcium and (b) phosphate ions into aqueous buffer from nACP particles, HA, nACP extracted from 30% nACP-PCL scaffold, control PCL scaffold and control 30% nACP-PCL scaffold (mean ± S.D., $n \geq 3$). Statistically significant differences ($p < 0.05$) are indicated by an asterisk (ANOVA with Tukey's). If an asterisk is encountered when following the line between two data points, then the data points are significantly different. All data are background subtracted for buffer controls where the experiment was conducted with buffer alone and no additives. Note that the concentrations of both calcium and phosphate ions released from HA particle and PCL scaffolds were not significantly higher than in buffer.

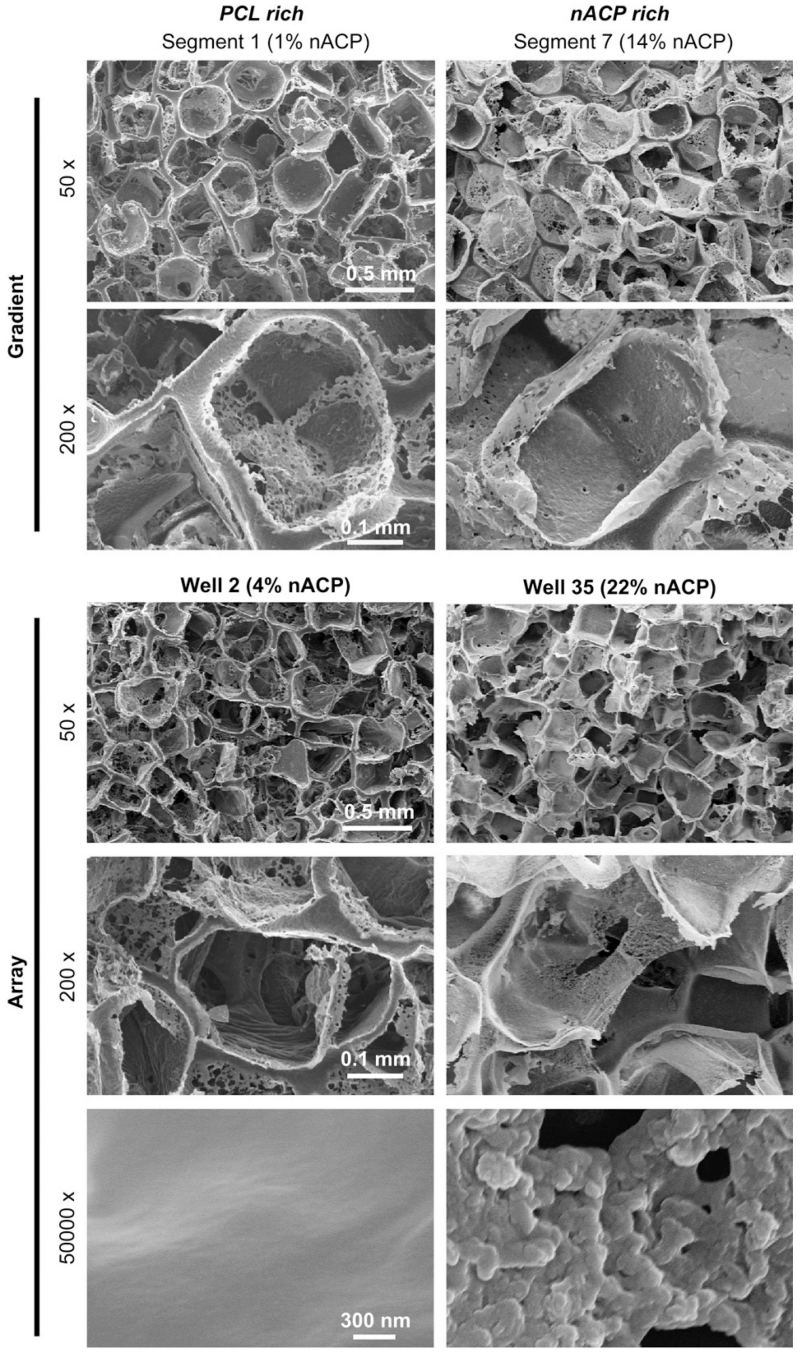

Fig. 5.

SEM of scaffolds from gradients and arrays at 50× and 200× magnification where left and right columns present PCL-rich and nACP-rich ends of the libraries, respectively. The bottom row is high magnification (50000×) showing the scaffold wall at the PCL-rich and nACP-rich ends of the arrays.

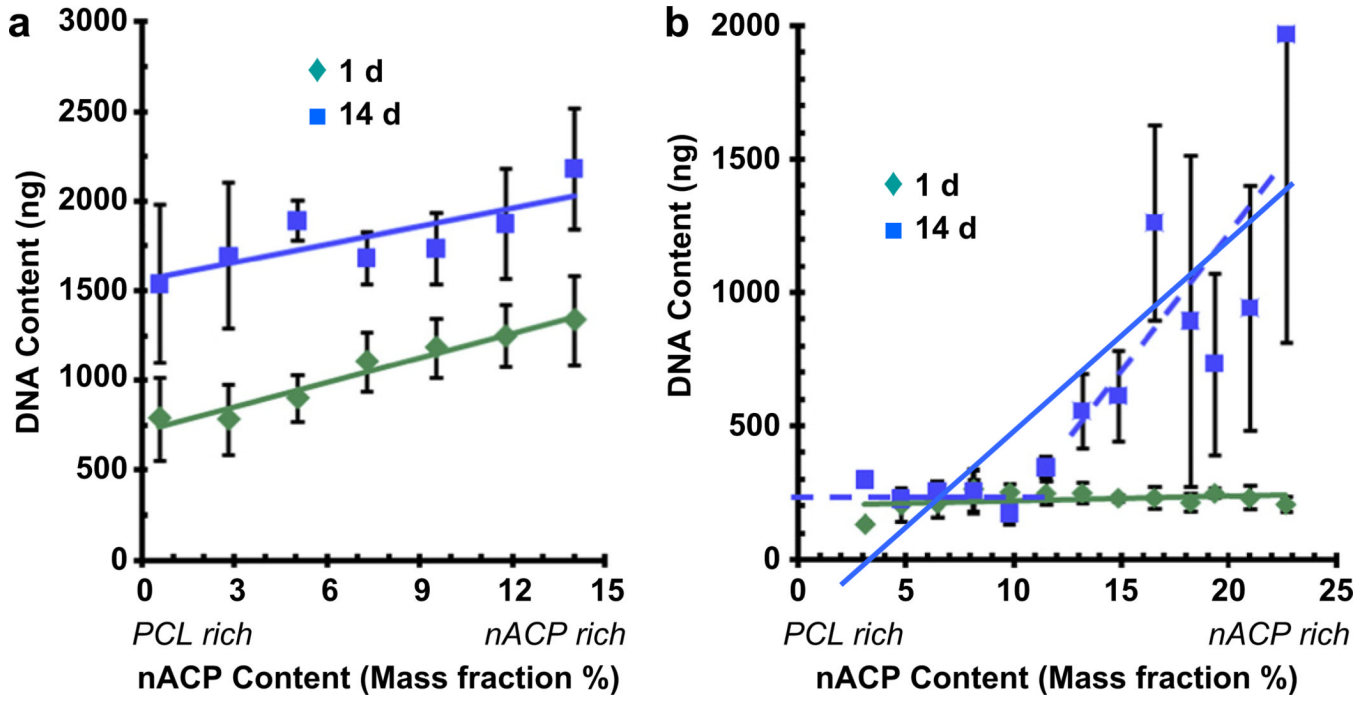

Fig. 6.

Cell number measured by DNA assay along the gradient (a) and array (b) libraries for 1 d (green diamonds) and 14 d (blue squares) culture of MC3T3-E1 osteoblasts (mean ± S.D., $n \geq 3$). (a) Slopes of the linear fits (green line for 1 d, blue for 14 d) are significantly greater than zero (*t*-test, $p<0.05$) at both 1 d and 14 d. Pearson correlation coefficients (R) were 0.98 for 1 d and 0.79 for 14 d. (b) Slope of the linear fit at 1 d (green line) was not significantly different from zero ($p<0.05$) but slope of fit at 14 d (solid blue line) was significantly greater than zero ($p<0.05$).For the 14 d data, a second analysis was included where separate fits were done for wells 1 (nACP 3%) to 18 (12%) and for wells 19 (13%) to 36 (23%) since there is a clear change in cell number at well 19. The well 1–18 slope was not significantly greater than zero ($p<0.05$) and the well 19–36 slope was significantly greater than zero ($p<0.05$). Pearson correlation coefficients (R) were 0.34 for 1 d, 0.82 for 14 d well 1–36 fit, 0.07 for 14 d well 1–18 fit and 0.70 for 14 d well 19–36 fit.

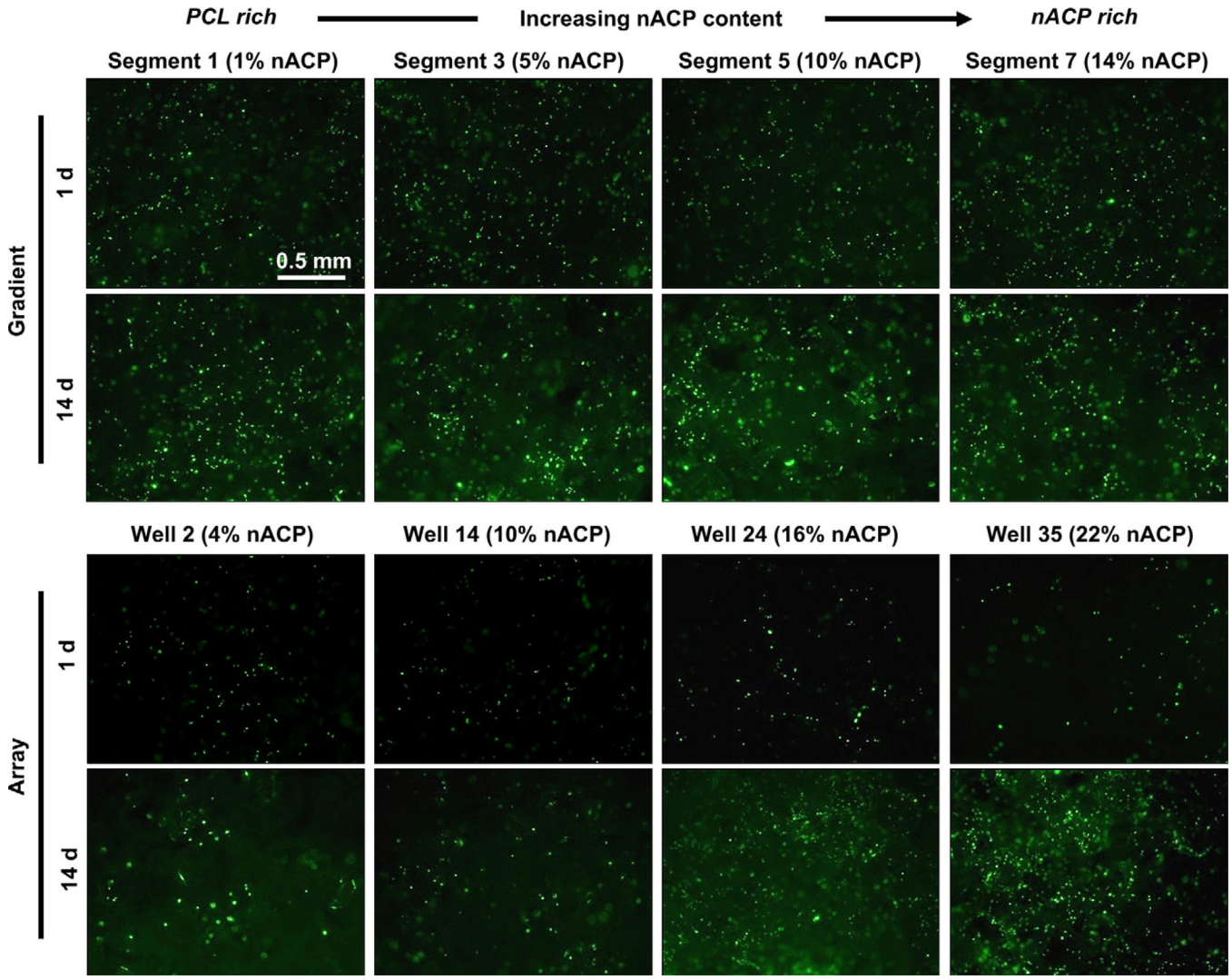

Fig. 7.

Fluorescent micrographs (40± magnification) of osteoblast nuclei (Sytox green) from gradient and array libraries after 1 d and 14 d culture. Scale bar applies to all images.